Journal of
Synchrotron
Radiation

ISSN 1600-5775

Received 22 April 2014
Accepted 23 June 2014

X-ray spectroscopy for chemical and energy sciences: the case of heterogeneous catalysis

Anatoly I. Frenkel[a]* and Jeroen A. van Bokhoven[b,c]*

[a]Department of Physics, Yeshiva University, 245 Lexington Avenue, New York, NY 10016, USA, [b]Department of Chemistry and Bioengineering, ETH Zürich, Wolfgang-Paulistrasse 10, Zürich 8093, Switzerland, and [c]Laboratory for Catalysis and Sustainable Chemistry, Paul Scherrer Institute, WLGA 135, Villigen 5232, Switzerland. *E-mail: anatoly.frenkel@yu.edu, jeroen.vanbokhoven@chem.ethz.ch

Heterogeneous catalysis is the enabling technology for much of the current and future processes relevant for energy conversion and chemicals synthesis. The development of new materials and processes is greatly helped by the understanding of the catalytic process at the molecular level on the macro/micro-kinetic time scale and on that of the actual bond breaking and bond making. The performance of heterogeneous catalysts is inherently the average over the ensemble of active sites. Much development aims at unravelling the structure of the active site; however, in general, these methods yield the ensemble-average structure. A benefit of X-ray-based methods is the large penetration depth of the X-rays, enabling *in situ* and *operando* measurements. The potential of X-ray absorption and emission spectroscopy methods (XANES, EXAFS, HERFD, RIXS and HEROS) to directly measure the structure of the catalytically active site at the single nanoparticle level using nanometer beams at diffraction-limited storage ring sources is highlighted. The use of pump–probe schemes coupled with single-shot experiments will extend the time range from the micro/macro-kinetic time domain to the time scale of bond breaking and making.

Keywords: heterogeneous catalysis; diffraction-limited storage rings; single-particle spectroscopy; time resolved; X-ray absorption; X-ray emission.

1. Introduction

Synchrotron-based investigations of low-dimensional nanomaterial, such as nanoparticles, nanowires and architectures of active sites is a rapidly developing field. One important reason for the ever-growing number of emerging characterization methods is the increased use of nanomaterials for energy generation, conversion and storage, in the pharmaceutical industry, biomedical engineering and environmental science. In catalysis, for example, new methods of synthesis create peculiar architectures that comprise a large variety of shapes, sizes and structural and compositional habits of nanocatalysts (Roldan Cuenya, 2012). These new capabilities in characterization and synthesis are paralleled by theoretical developments. This opens opportunities to rationally predict catalytic activity and selectivity by tailoring structure to the desired catalytic function.

Modern applications of synchrotron-based X-ray absorption (XAS) and emission (XES) spectroscopy methods of active site characterization are performed *in situ*, where the catalysts are studied under realistic temperature and pressure conditions (Frenkel *et al.*, 2012; Bordiga *et al.*, 2013; de Groot, 2001; Glatzel & Bergmann, 2005; Singh *et al.*, 2010a; Garino *et al.*, 2014). Often, their mechanism of work can be understood only if they are investigated *operando*, *i.e.* while working. This approach is particularly powerful because it correlates real time characterization of working catalysts with the corresponding changes in reactants and products measured simultaneously. XAS and XES probe the local structure in an element-specific manner. Complementary measurements, such as X-ray diffraction and vibrational spectroscopies, such as UV–visual light, IR and Raman, offer complementary information on the long-range order and that on intermediates (Stavitski & Weckhuysen, 2010; Bentrup, 2010). Combining methods is essential for analysing complex multi-component systems (Frenkel *et al.*, 2011, 2012; Bordiga *et al.*, 2013). In the last decade, the ability to characterize electronic states of the catalysts and their interactions with adsorbates has been dramatically improved due to the developments of new secondary emission and high-energy-resolution experiments (HERFD) (Hämäläinen *et al.*, 1991; Safonova *et al.*, 2006; Pushkar *et al.*, 2007; Yano *et al.*, 2005, 2008; Glatzel *et al.*, 2010), resonant inelastic X-ray scattering (RIXS) (Glatzel *et al.*, 2010; Glatzel & Bergmann, 2005) and high-energy-resolution off-resonant spectroscopy (HEROS) (Szlachetko *et al.*, 2012; Kavčič *et al.*, 2013).

The developments in synthesis, characterization and modeling methods, accompanied by the advancements in first-principle theories to model X-ray absorption and emission spectra, offer high accuracy of structural refinement, sufficient to discriminate between the details of particle structure (*e.g.* cuboctahedral or icosahedral), shapes, support orientation and details of multi-metallic and multi-oxide compositions (Frenkel, 2012) (*e.g.* core/shell, cluster-to-cluster or random alloy or oxide). The more accurate the structural methods become, the more obvious becomes their main limitation: artefacts due to the ensemble averaging (Yevick & Frenkel, 2010; Frenkel *et al.*, 2013*a*). In contrast to homogeneous and enzymatic catalysts, heterogeneous ones possess inherent structural heterogeneities due to the distributions of cluster sizes and shapes within the sample. Studies of the architecture and electronic properties of nanocatalysts by X-ray absorption are hindered by the ensemble-averaging nature of this technique, posing a real challenge when its results are compared with first-principles theories that investigate a 'representative catalytic particle or active site'. Time-resolution at the macrokinetic time scale, using, for example, gas switching, and at the ultrafast scale, using pump–probe, will yield relationships between performance on the one side and structure and structural changes that occur during individual reaction steps on the other. *Operando* studies at the single-nanoparticle level will allow the structure and electronic properties to be directly evaluated, and their relation to catalytic performance as probed in real time, in the same spectroscopy experiment. Diffraction-limited storage ring (DLSR) sources ultimately hold the promise to measure individual particles or parts of larger units and selectively detect the structure of a functioning catalyst in real time.

2. Single nanoparticle spectroscopy: *in situ* and *operando*

Optical spectroscopy experiments focused on characterizing single nanoparticles range from spatial modulation spectroscopy (Arbouet *et al.*, 2004; Muskens *et al.*, 2008) to the high spectral resolution flow spectroscopy (Sebba *et al.*, 2009) to surface-enhanced Raman scattering (Nie & Emory, 1997) and single-molecule spectroscopy (Xu *et al.*, 2008). P. Chen's group used detection of fluorescence of catalytic products in fluoregenic reactions to provide the basis for real time studies of single nanoparticle catalysis at the single-molecule level (Xu *et al.*, 2008, 2009; Zhou *et al.*, 2009). They discovered that colloidal Au nanoparticles of 6 nm in size (on the average) fall into two distinct groups, type-a and type-b, with respect to their catalytic properties of reducing resazurin to resorufin (Xu *et al.*, 2009). It is the heterogeneity in distribution of Au nanoparticle sizes and shapes that was responsible for the two types of catalysts, presumably due to the different percentages of corner, edge and facet atoms (Xu *et al.*, 2009). Catalytic activity measured on each particle type differs: type-a sites have stronger substrate binding with lower reactivity and type-b sites have weaker substrate binding with higher reactivity. This work demonstrated the benefit that single-nanoparticle spectroscopy offers in determining catalytic mechanisms and the limitations of the ensemble-averaging techniques that give only average values of relevant kinetic parameters.

2.1. X-ray spectroscopy at the single-particle level: current state of the art

The article by A. Hitchcock and M. Toney in this issue (Hitchcock & Toney, 2014) gives an overview of spectro-microscopy methods that include nanoprobe-based systems. An illustration of the capability of nanoprobe methods for spectroscopy studies of single nanoparticles is the work from Y. Chu's group from Brookhaven National Laboratory (BNL). They demonstrate that a composition of individual bimetallic nanoparticles (NPs) in the size range between 140 and 320 nm can be studied by X-ray fluorescence (Kang *et al.*, 2013). They used scanning multilayer Laue lens (MLLs) X-ray microscopy to study the oxidation process of individual PtNi nanoparticles. This experiment was performed at beamline 26ID of the Advanced Photon Source at Argonne National Laboratory. The smallest core size of the Pt/NiO core-shell NPs was ~40 nm, and the scanning was performed with 10 nm step size and 30 nm focal spot size. The methods described by Y. Chu *et al.* will be used at the hard X-ray nanoprobe (HXN) beamline of the National Synchrotron Light Source II (NSLS-II) at BNL.

Rodríguez *et al.* (2007) demonstrated that individual cobalt nanoparticles of the sizes ~8 nm can be probed by XAS in a photoemission electron microscopy (PEEM) experiment. Significant variations in the shapes of the Co $L_{2,3}$ edges of the X-ray absorption spectra between different cobalt nanoparticles were detected (Fig. 1) and attributed to different cobalt–oxygen interactions on a particle-by-particle basis.

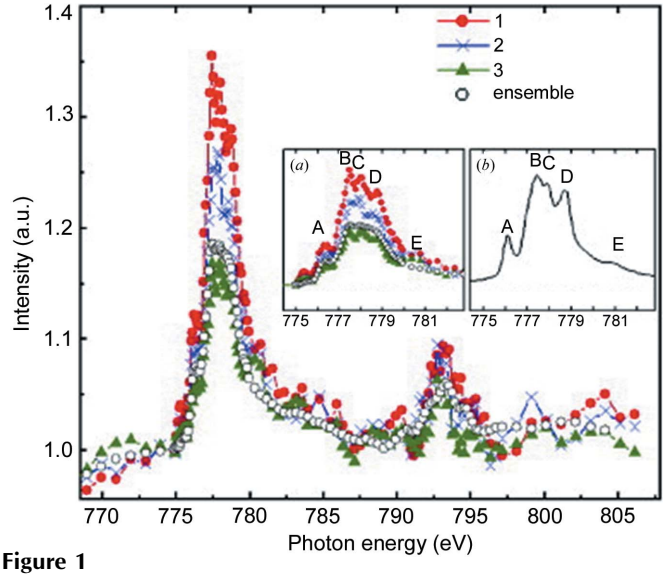

Figure 1
X-ray absorption spectra at the Co $L_{2,3}$-edges as a function of the incident X-ray energy of three different cobalt particles of ~8 nm in diameter. The insets compare (*a*) the L_3 peak region of the particles with (*b*) the L_3-edge peak region of a reference CoO film. The spectrum with open circles in (*a*) represents the average of the X-ray absorption spectra of 23 different nanoparticles. [From *J. Magn. Magn. Mater.* **326**, 426–428, Rodríguez *et al.* (2007). Copyright (2007), with permission from Elsevier.]

2.2. Challenges and limitations for catalytic investigations

The main challenge in the existing nanoprobe methods is to decrease the spot size to well below 10 nm while maintaining sufficiently high flux to probe individual nanoparticles of interest to catalytic applications. MLLs are a novel type of diffractive nanofocusing optics that are capable of achieving, in principle, such spot sizes and high efficiency in the hard X-ray range (Kang *et al.*, 2013). Another challenge is to enable energy scanning while maintaining the spot size and position. Current fluorescent imaging capabilities are based on selecting a particular X-ray wavelength for mapping the bimetallic composition within an individual particle but they are not generally sufficient for analysing the chemical state of each element usually done by XANES or the nature of structure and dynamics of its local environment from EXAFS data. Indeed, existing nanoprobe-based methods can be used predominantly for chemical speciation and, to a limited degree, reveal sensitivity to environmental effects (Rodríguez *et al.*, 2007). There is a distinct need to move experimental capabilities to the next level of detail. For example, nanoparticles with different sizes and shapes have different metal–metal bond lengths, lattice terminations and surface defects and, hence, different catalytic properties. Structural and electronic characterization of three-dimensional geometry by single-nanoparticle spectroscopy (XANES and EXAFS) can obtain precisely this type of information. We note in this regard that current experiments with particles of 100 nm in size allow, in principle, both the chemical state and crystal structure determination by coupling X-ray fluorescence with X-ray diffraction from the same particle (Kang *et al.*, 2013) but the latter method cannot be applied to particles of several nanometers in diameter. Strong particle size effects in structure and catalytic performance are generally observed for particles smaller than 5 nm, which illustrates the challenge ahead (Haruta, 1997; Miller *et al.*, 2006).

An additional challenge, as we emphasized in the *Introduction*, is the need to study materials that change in the process of their work and, hence, single-particle spectroscopy at the nanometer level should be performed in *operando* conditions. That requirement constrains X-ray experiments studying such processes to be performed on samples placed in specially designed *operando* reactors where temperature, pressure and/or potentiostatic control are enabled. Currently developed reactors and devices are not yet compatible with the small focal distances (of the order of 1 mm) of the nanoprobe, and future work is needed to bridge this instrument gap for studying single particles *in situ* or *operando* by nanoprobe methods.

3. Time-resolved spectroscopy for active site and mechanism determination

There are three fundamental requirements for a catalytic reaction to occur. The first is adsorption of the reactant to the catalyst surface, the second the surface reaction, and the third desorption of the product. All three steps must be completed for a catalytic cycle to occur and repeat itself. The function of the catalyst is to break bonds and to make bonds, which it does by forming strong chemisorbed bonds with reaction intermediates. This strong bonding affects electronic structure and often oxidation state and geometric structure of the catalytically active site. This makes characterization under catalytically relevant conditions essential. Measuring catalysts *ex situ*, before or after, likely misses the essence of the catalytic reaction. However, the catalytic site in a heterogeneous catalyst constitutes the minority of all atoms. Capturing the structure of exactly these atoms requires measuring in the time domain, for example, in transient conditions or by pump–probe schemes.

3.1. Current state of the art

The principle of measuring active sites under transient conditions is that after switching conditions, such as a sudden change in gas composition or temperature, the catalytically active site changes structure with a different rate as that of the spectator and non-active sites. An early example was performed in the group of T. Oyama in collaboration with M. Haruta, who measured transient XANES at the Ti *K*-edge to determine the rate of Ti-hydroperoxo formation during the gas-phase epoxidation of propylene with hydrogen and oxygen (Bravo-Suárez *et al.*, 2008). The catalyst was a Au-Ba/Ti-SiO_2. A pre-edge feature was used to quantify the coverage of the hydroperoxo and the transient conditions enabled measuring their rate of reaction, which had the same order of magnitude as the steady-state rate of propylene epoxidation. This established the hydroperoxo species as unambiguously as a reaction intermediate and illustrated that time-resolved XAS can be used to measure catalytically relevant rates. Although we only discussed their XAS data, complementary data were reported using *in situ* UV–visible and infrared spectroscopies.

A second example by J. Singh *et al.* illustrates that subtle changes in the reaction conditions may cause large changes in catalyst structure, paralleled by changes in catalytic performance. In a plug-flow reactor, the platinum structure was determined while it oxidized carbon monoxide. The typical light-off and oscillating behavior of this reaction was observed, during which a rapid increase in rate of reaction occurs when surplus of oxygen is present at the surface of the catalyst (Singh *et al.*, 2008, 2010*b*). The structure of the catalyst was strongly changing with reaction conditions, yielding low and high activities of the catalyst. The structure of the catalyst varied within the same catalyst bed, because of the different local conditions that originate from the catalytic conversion. The surfaces of the nano-sized platinum particles were covered with and poisoned by carbon monoxide generating the low active catalyst. Upon increasing conversion, the oxygen concentration at the catalyst surface increases and a switch to a more reactive surface occurs; *via* an intermediate state, the more active distorted surface oxide forms. Under oscillating conditions, the relative amounts of species fluctuates accordingly (Fig. 2). The relative ratio of high-activity

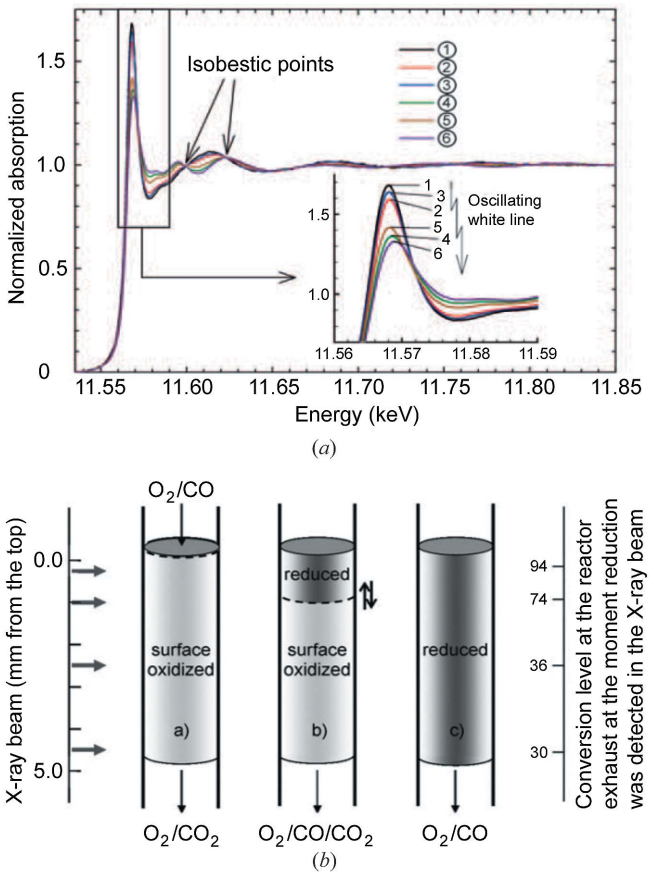

Figure 2
Oscillations in the white-line intensity were observed during fluctuating rates of carbon monoxide oxidation (*a*). Higher intensity indicates a larger fraction of distorted surface oxide relative to the low-activity carbon-monoxide-poisoned state. The relative amounts of catalyst with surface oxide (high rate) and catalyst poisoned with carbon monoxide (low rate) determine the overall rate of reaction (*b*). The amounts change over time and as function of position within the reactor. [From Singh *et al.* (2010*b*). Copyright: *ChemCatChem*, 2010.]

and low-activity catalyst within a single reactor determines the overall oxidation rate.

These examples illustrate that, upon changing conditions, the response of the catalyst captures the structure of the changing active site. The time-resolved nature of the measurements is essential to capture these changes. An intrinsic limitation of XAS and XES methods is their quantitative nature: at any absorption edge, all atoms constituting that edge contribute to the spectroscopic signature, which is thus an average of all species. The above-mentioned experiments circumvent this by measuring the change in structure of the active site. However, as the catalytically active site is often only a minority of atoms in the catalyst, sensitivity is an issue. The recently introduced modulation excitation and filtering the corresponding spectra with the excitation frequency has increased the sensitivity to the differences in the spectra (Ferri *et al.*, 2010, 2011, 2013) thus promising to capture the structure of the active site selectively (Ferri *et al.*, 2011; Konig *et al.*, 2012). Intermediate species can be detected by a phase delay of the structural difference.

Pump–probe measurements are able to capture structural variation at the micro-, nano-, pico- and even femtosecond time scales (Bressler & Chergui, 2004). Most of the examples in the literature relate to photocatalytic processes during which a flash of light induces electron excitation after which a structure change occurs that is detected in the ultrafast time domain. An illustrative example is that of Chergui *et al.* (Bressler *et al.*, 2009) who measured the ultrafast formation of the lowest quintet state of aqueous iron(II) tris(bipyridine) upon excitation of the singlet metal-to-ligand charge-transfer (1MLCT) state by femtosecond optical-pump–X-ray-probe (Lima *et al.*, 2011). By recording the intensity of the characteristic XANES feature as a function of laser-pump–X-ray-probe time delay, the population of the quintet state occurred in about 150 fs. These results resolved the long-standing issue about the population mechanism of quintet states in iron(II)-based complexes: a simple 1MLCT $\rightarrow$ 3MLCT $\rightarrow$ 5T cascade from the initially excited state occurs. The time scale of the 3MLCT $\rightarrow$ 5T relaxation corresponds to the period of the iron–nitrogen stretch vibration.

Many macro- and micro-kinetic chemical processes that occur during photocatalysis are slower, and measuring with less-demanding time resolution is sufficient. Efficient water-splitting catalysts are essential to convert solar energy into chemicals, initially hydrogen and oxygen. Their functioning must be improved and large efforts are given to understanding the processes that occur during and directly after light excitation. Smolentsev *et al.* developed a detection scheme to determine the structure of cobalt reaction intermediates of a hydrogen formation catalytic system consisting of multi-components $Co(dmgBF_2)_2$ catalyst (dmg^{2-} = dimethylglyoximato dianion), $[Ru(bpy)_3]^{2+}$ chromophore (bpy = 2,2′-bipyridine) and methyl viologen as the electron relay. In the microsecond time domain a Co(I) intermediate was identified with the aid of theoretical spectral simulation. The change in oxidation state was paralleled by local structural variation (Smolentsev *et al.*, 2014). Understanding the reaction mechanism helps the design of better and more stable catalysts.

Molecular structure and electronic change is accessible at the micro-, nano-, pico- and even femtosecond time scale in pump–probe schemes, making them highly attractive for measuring individual reaction steps. These experiments are photon-hungry and most examples to date are performed in a liquid jet, because of the continuous refreshing of sample. Significant challenges and opportunities lie ahead to measure single particles in a pump–probe scheme.

4. New opportunities at the diffraction-limited storage ring sources

Measuring at the micro/macro-kinetic time scale enables spectator species to be distinguished from those that actively participate in a reaction. The measurements in the ultrafast time domain will unravel individual and fundamental reaction steps. These emerging and rapidly developing tools hold the promise to, for the first time, disentangle not only the structure

of the active site but also the structural changes that the site undergoes during the catalytic cycle, thus contribute to unravelling the reaction mechanism. These complex measurements and establishing structure–performance relationships are greatly helped by the ability to measure single particles, thus removing the inherent complexity of heterogeneity and measuring a structure ensemble. Despite the large progress in the ability to control structure at the molecular level, monodispersion of active site structure and composition has not been achieved for heterogeneous catalysts. Time-resolved structural changes of individual particles and sites must be related to the micro/macro-kinetic parameters of the catalytic reaction to ensure relevance of the spectroscopic measurement.

Nanometer-size beams produced by the DLSR source will carry the same flux as the beams used at existing synchrotrons. A coherent flux produced by a DLSR on a square nanometer on the sample will be comparable with the flux on a square micrometer in many existing third-generation sources. Hence, X-ray spectroscopy experiments with single nanoparticles can be envisioned (Fig. 3). In such hypothetical experiments, XANES and EXAFS data will provide information about the local coordination environment of different types of atoms in a particle (on the surface, near support or in the core) as well as the overall structure, size and shape of individual particles (Fig. 3*a*). Complementary X-ray emission, HERFD and HEROS data will provide the details of the particle–adsorbate and particle–support interactions (Safonova *et al.*, 2006; Glatzel *et al.*, 2010; Szlachetko *et al.*, 2012; Frenkel *et al.*, 2013*b*). RIXS experiments with individual nanoparticles, described by T. Schmitt *et al.* in this issue (Schmitt *et al.*, 2014), will complement XANES and EXAFS by providing information about local chemistry of the particle–adsorbate–support interaction (Small *et al.*, 2014) or real time changes in the oxidation state of the catalyst (Szlachetko *et al.*, 2013) through the measurement of the electronic structure of the individual catalysts during the catalytic reaction. Methods that are based on single-shot detection, thus using monochromatic X-rays and detecting X-ray emission in a single shot, are attractive as the X-ray beam is not affected by any moving optical component thus simplifying the measurement scheme.

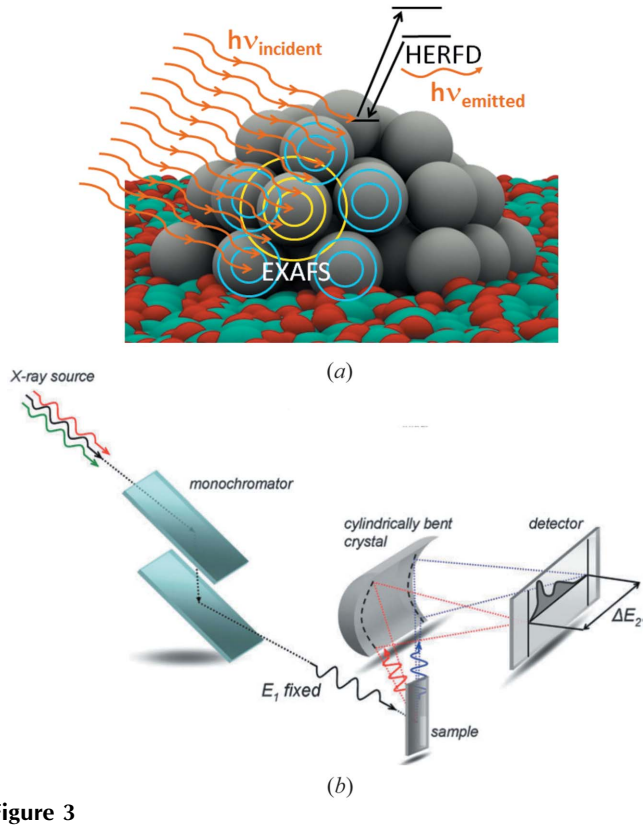

Figure 3
Two possible X-ray spectroscopy experiments with single nanoparticles. (*a*) Using EXAFS to study local structure, size and shape in a supported Pt nanoparticle by EXAFS and its chemical state and interactions with adsorbates and support by HERFD. [Modified from Frenkel *et al.* (2013*b*). Copyright: American Chemical Society, 2013.] (*b*) Using *in situ*/*operando* single-shot experiments to study real time changes in electronic properties of single nanoparticle catalyst in reaction conditions. [From Szlachetko *et al.* (2012). Copyright: Royal Society of Chemistry, 2012.]

5. Conclusions

As experimental infrastructure in catalysis science becomes more advanced and now features such innovations as combining multiple techniques in a single experiment, as well as *operando* research methods, the common limitation of most such methods due to the heterogeneity of model and real catalysts will continue to hamper the progress in understanding catalytic mechanisms at the atomistic level. In this article we outlined several new opportunities for catalysis science at diffraction-limited storage ring sources that will help better understand the details of catalytically active sites due to the high flux carried by nanometer beams. We emphasized advanced spectroscopy applications (such as HEROS) that can be used with equal facility to study either steady-state or time-resolved (including ultrafast) chemical transformations. In the space domain, we envision that the DLSR sources will enable studies of catalytic processes at the single-nanoparticle level by XANES, EXAFS and RIXS methods.

AIF acknowledges support by the US Department of Energy Grant No. DE-FG02-03ER15476.

References

Arbouet, A., Christofilos, D., Del Fatti, N., Vallée, F., Huntzinger, J. R., Arnaud, L., Billaud, P. & Broyer, M. (2004). *Phys. Rev. Lett.* **93**, 127401.
Bentrup, U. (2010). *Chem. Soc. Rev.* **39**, 4718–4730.
Bordiga, S., Groppo, E., Agostini, G., van Bokhoven, J. A. & Lamberti, C. (2013). *Chem. Rev.* **113**, 1736–1850.
Bravo-Suárez, J. J., Bando, K. K., Lu, J., Haruta, M., Fujitani, T. & Oyama, T. (2008). *J. Phys. Chem. C*, **112**, 1115–1123.
Bressler, C. & Chergui, M. (2004). *Chem. Rev.* **104**, 1781–1812.
Bressler, C., Milne, C., Pham, V.-T., Elnahhas, A., van der Veen, R. M., Gawelda, W., Johnson, S., Beaud, P., Grolimund, D., Kaiser, M., Borca, C. N., Ingold, G., Abela, R. & Chergui, M. (2009). *Science*, **323**, 489–492.
Ferri, D., Kumar, M. S., Wirz, R., Eyssler, A., Korsak, O., Hug, P., Weidenkaff, A. & Newton, M. A. (2010). *Phys. Chem. Chem. Phys.* **12**, 5634–5646.

Ferri, D., Newton, M. A., Di Michiel, M., Yoon, S., Chiarello, G. L., Marchionni, V., Matam, S. K., Aguirre, M. H., Weidenkaff, A., Wen, F. & Gieshoff, J. (2013). *Phys. Chem. Chem. Phys.* **15**, 8629–8639.
Ferri, D., Newton, M. A. & Nachtegaal, M. (2011). *Top. Catal.* **54**, 1070–1078.
Frenkel, A. I. (2012). *Chem. Soc. Rev.* **41**, 8163–8178.
Frenkel, A. I., Rodriguez, J. A. & Chen, J. G. (2012). *ACS Catal.* **2**, 2269–2280.
Frenkel, A. I., Small, M. W., Smith, J. G., Nuzzo, R. G., Kvashnina, K. O. & Tromp, M. (2013*b*). *J. Phys. Chem. C*, **117**, 23286–23294.
Frenkel, A. I., Wang, Q., Marinkovic, N., Chen, J. G., Barrio, L., Si, R., Cámara, A. L. p., Estrella, A. M., Rodriguez, J. A. & Hanson, J. C. (2011). *J. Phys. Chem. C*, **115**, 17884–17890.
Frenkel, A. I., Wang, Q., Sanchez, S. I., Small, M. W. & Nuzzo, R. G. (2013*a*). *J. Chem. Phys.* **138**, 064202.
Garino, C., Borfecchia, E., Gobetto, R., van Bokhoven, J. A. & Lamberti, C. (2014). *Coord. Chem. Rev.* In the press.
Glatzel, P. & Bergmann, U. (2005). *Coord. Chem. Rev.* **249**, 65–95.
Glatzel, P., Singh, J., Kvashnina, K. O. & van Bokhoven, J. A. (2010). *J. Am. Chem. Soc.* **132**, 2555–2557.
Groot, F. de (2001). *Chem. Rev.* **101**, 1779–1808.
Hämäläinen, K., Siddons, D. P., Hastings, J. B. & Berman, L. E. (1991). *Phys. Rev. Lett.* **67**, 2850–2853.
Haruta, M. (1997). *Catal. Today*, **36**, 153–166.
Hitchcock, A. P. & Toney, M. F. (2014). *J. Synchrotron Rad.* **21**, 1019–1030.
Kang, H. C., Yan, H., Chu, Y. S., Lee, S. Y., Kim, J., Nazaretski, E., Kim, C., Seo, O., Noh, D. Y., Macrander, A. T., Stephenson, G. B. & Maser, J. (2013). *Nanoscale*, **5**, 7184–7187.
Kavčič, M., Žitnik, M., Bučar, K., Mihelič, A., Marolt, B., Szlachetko, J., Glatzel, P. & Kvashnina, K. (2013). *Phys. Rev. B*, **87**, 075106.
Konig, C. F. J., van Bokhoven, J. A., Schildhauer, T. J. & Nachtegaal, M. (2012). *J. Phys. Chem. C*, **116**, 19857–19866.
Lima, F. A., Milne, C. J., Amarasinghe, D. C. V., Rittmann-Frank, M. H., van der Veen, R. M., Reinhard, M., Pham, V.-T., Karlsson, S., Johnson, S. L., Grolimund, D., Borca, C., Huthwelker, T., Janousch, M., van Mourik, F., Abela, R. & Chergui, M. (2011). *Rev. Sci. Instrum.* **82**, 063111.
Miller, J. T., Kropf, A. J., Zha, Y., Regalbuto, J. R., Delannoy, L., Louis, C., Bus, E. & van Bokhoven, J. A. (2006). *J. Catal.* **240**, 222–234.
Muskens, O. L., Billaud, P., Broyer, M., Del Fatti, N. & Vallée, F. (2008). *Phys. Rev. B*, **78**, 205410.
Nie, S. & Emory, S. R. (1997). *Science*, **275**, 1102–1106.
Pushkar, Y., Yano, J., Glatzel, P., Messinger, J., Lewis, A., Sauer, K., Bergmann, U. & Yachandra, V. (2007). *J. Biol. Chem.* **282**, 7198–7208.
Rodríguez, A. F., Nolting, F., Bansmann, J., Kleibert, A. & Heyderman, L. (2007). *J. Magn. Magn. Mater.* **316**, 426–428.
Roldan Cuenya, B. (2012). *Acc. Chem. Res.* **46**, 1682–1691.
Safonova, O. V., Tromp, M., van Bokhoven, J. A., de Groot, F. M. F., Evans, J. & Glatzel, P. (2006). *J. Phys. Chem. B*, **110**, 16162–16164.
Schmitt, T., de Groot, F. M. F. & Rubensson, J.-E. (2014). *J. Synchrotron Rad.* **21**, 1065–1076.
Sebba, D. S., Watson, D. A. & Nolan, J. P. (2009). *ACS Nano*, **3**, 1477–1484.
Singh, J., Alayon, E. M. C., Tromp, M., Safonova, O. V., Glatzel, P., Nachtegaal, M., Frahm, R. & van Bokhoven, J. A. (2008). *Angew. Chem. Int. Ed.* **47**, 9260–9264.
Singh, J., Lamberti, C. & van Bokhoven, J. A. (2010a). *Chem. Soc. Rev.* **39**, 4754–4766.
Singh, J., Nachtegaal, M., Alayon, E. M. C., Stötzel, J. & van Bokhoven, J. A. (2010b). *ChemCatChem*, **2**, 653–657.
Small, M. W., Kas, J. J., Kvashnina, K. O., Rehr, J. J., Nuzzo, R. G., Tromp, M. & Frenkel, A. I. (2014). *Chem. Phys. Chem.* **15**, 1569–1572.
Smolentsev, G., Guda, A., Janousch, M., Frieh, C., Jud, G., Zamponi, F., Chavarot-Kerlidou, M., Artero, V. & Van Bokhoven, J. A. (2014). *Faraday Discuss.* doi:10.1039/C4FD00035H.
Stavitski, E. & Weckhuysen, B. M. (2010). *Chem. Soc. Rev.* **39**, 4615–4625.
Szlachetko, J., Nachtegaal, M., Sá, J., Dousse, J.-C., Hoszowska, J., Kleymenov, E., Janousch, M., Safonova, O. V., König, C. & van Bokhoven, J. A. (2012). *Chem. Commun.* **48**, 10898–10900.
Szlachetko, J., Sá, J., Safonova, O. V., Smolentsev, G., van Bokhoven, J. A. & Nachtegaal, M. (2013). *J. Electron Spectrosc. Relat. Phenom.* **188**, 161–165.
Xu, W., Kong, J. S. & Chen, P. (2009). *Phys. Chem. Chem. Phys.* **11**, 2767–2778.
Xu, W., Kong, J. S., Yeh, Y.-T. & Chen, P. (2008). *Nat. Mater.* **7**, 992–996.
Yano, J., Kern, J., Pushkar, Y., Sauer, K., Glatzel, P., Bergmann, U., Messinger, J., Zouni, A. & Yachandra, V. K. (2008). *Philos. Trans. R. Soc. B*, **363**, 1139–1147.
Yano, J., Pushkar, Y., Glatzel, P., Lewis, A., Sauer, K., Messinger, J., Bergmann, U. & Yachandra, V. (2005). *J. Am. Chem. Soc.* **127**, 14974–14975.
Yevick, A. & Frenkel, A. I. (2010). *Phys. Rev. B*, **81**, 115451.
Zhou, X., Xu, W., Liu, G., Panda, D. & Chen, P. (2009). *J. Am. Chem. Soc.* **132**, 138–146.